A Low-Cost, Non-Contact, Optical Imaging Pulse-Oximeter System

By Alexa Christine Romero

Senior Honors Thesis

Department of Biomedical and Health Science Engineering

University of North Carolina at Chapel Hill

March 30, 2018

Approved:

_____

Devin Hubbard, Thesis Advisor

Kenneth Donnelly, Reader

Naji Husseini, Reader

Acknowledgments

To my parents Christine and Tony Romero: because I owe it all to you two. A Million Thanks!

To my strong and honest siblings, Natalie and Tony: I do not think you realize how much I look up to you both. You remind me to appreciate obstacles and never stop learning.

An enormous thank-you to my friends at UNC Chapel Hill for supporting me through my stress-induced, emotional rollercoaster.

A very special gratitude to the Tom and Elizabeth Long Research Foundation for funding the work and allowing me to achieve this amazing feat.

And finally, last but most important, I am so thankful for the mentorship and friendship of my thesis advisor, Dr. Devin Hubbard. You have pushed me to believe in myself and provided me with the tools to feel secure in my abilities as I move forward in my professional career.

Thanks for all your encouragement!

Table of Contents

Abstract

This thesis proposed the design and construction of a low-cost, non-contact, optical imaging system capable of data acquisition useful in calculating blood oxygenation and heart rate. This system essentially behaves the same way as traditional pulse-oximetry, with the modifications that it acts at a distance and calculates oxygenation over the pixels of an image rather than from a single photo-transducer. The system illuminates the human forearm with 660nm and 910nm wavelengths independently and acquires high frequency images at these two wavelengths. This allows for resolution of two distinct, wavelength-dependent absorption curves. The system is capable of measuring statistically significant changes in light absorption of biological tissue over time ($p\text{-value}<0.05$). By performing single and multi pixel analysis over images acquired at a high enough frequency to resolve pulsatile information the system is capable of perfusion mapping. The highly vascularized imaged area are highlighted by the system, illustrating vein location and increased blood flow. Issues with synchronizing the high frequency image acquisition with the illumination switching limited the system's ability to produce measurements required for blood oxygen calibration techniques. Further research should be performed to analyze the depth capabilities of the system and whether it can be applied to areas other than the forearm.

1 Introduction

Sufficient oxygenation of tissue is a prerequisite for successful wound healing due to the increased energy expenditure during the cellular reparative processes [1]. The current technologies used to compute blood oxygenation require direct contact with patients to measure the oxygenation of arterial blood. The current technology requires a sensor to be placed on a small area on the body (usually a finger or earlobe), and thus only provides information about a single, relatively unfocused area and reveals nothing about blood flow in surrounding areas [2]. Additionally, the physical contact required makes current techniques inappropriate for use in assessing sensitive dermal conditions such as burns. This thesis project proposes an optically based system capable of obtaining the data required to calculate superficial blood oxygenation and perfusion without direct contact with dermal tissue. The work completed provides preliminary data for future research into non-contact pulse-oximetry technology. This device will ultimately allow blood oxygen saturation measurements to be made non-invasively from a distance, which is especially useful in burn patients, isolating them from the high infection risk with dermal contact.

2 Background

To measure blood oxygen saturation, traditional pulse-oximetry technology attempts to find the concentrations of deoxygenated hemoglobin (Hb) and oxygenated hemoglobin (HbO_2) in the blood. There are two unknown concentrations of these two states of hemoglobin that both contribute to the overall absorption signal. To find the individual concentrations, two absorption equations are required.

Because Hb and HbO_2 absorb certain wavelengths of light differently, pulse-oximeters make use of absorption properties to calculate the oxygen saturation (SaO_2) of blood. Beer-Lambert's Law shows that the incident and transmitted light intensity are logarithmically related to the absorbance of the solution [3]:

$$\boldsymbol{I_{transmitted} = I_{incident}\, e^{-dC\epsilon}}$$

(Eq 1)

where d is the path length, C is the concentration of the solute, and ϵ is the extinction coefficient (molecular property of light absorption of the solute which is constant at a given wavelength). These equations relate the wavelength of transmitted light to the amount of incident light measured for a specific substance [3]. To calculate SaO_2, the total amount of Hb and HbO_2 must be found:

$$SaO_2 = \frac{HbO_2}{HbO_2 + Hb} x100\%$$

(Eq 2)

Two wavelengths that are absorbed by HbO_2 and Hb differently are used to create two curves. The curves, comprised of the electrical output of the phototransistors have AC (alternating

current) and DC (direct current) components. Current technology then commonly uses the ratio of ratios (RoR), described by:

$$R = \frac{AC_{660nm}/DC_{660nm}}{AC_{910nm}/DC_{910nm}} \quad \text{(Eq 3)}$$

to find the ratio of the two curves constructed at different wavelengths, which then is calibrated to a corresponding SaO_2 value [3].

The proposed system uses the same lighting technique of current technologies by illuminating the subject with two light emitting diodes (LEDs) with wavelengths that are absorbed differently by Hb and HbO_2. The non-contact system differs by using a camera allowing for multi-pixel analysis instead of a single phototransistor. The traditional technology requires contact with the skin at a known path length (emitter to transistor). The non-contact will occur at an unknown distance from the subject, which will need to be measured for data calculation. A Time-of-Flight (TOF) sensor will be used in the system to correct for distance.

Oxygen is extremely important in maintaining cell function [4]. Pulse-oximetry allows for real-time measurement of arterial blood oxygen saturation providing important information about the patient. Not only will this system provide the ability to gauge bulk cellular perfusion, because wounds require an increase in oxygen levels, but the pulse-oximeter can be also be used to measure SaO_2 in the areas surrounding a wound, making it a useful clinical tool for assessing wound healing. For wounds that are covered by scabs or scars, the wavelengths chosen could penetrate below the surface of the wound. The pulse-oximeter can also measure other medical vitals from sub-dermal blood flow such as heart rate. Pulse can be extracted from the data acquired by the pulse-oximeter due to the change in absorbance of emitted light as blood is

pushed through the arterial pathways. This allows for blood flow in specific areas of the body (possibly a wound site) to be measured and potentially visualized in real time.

3 Methodology

3.1 Synchronous high-frequency illuminated image acquisition

3.1.1 Design a synchronous LED source appropriate for measuring blood oxygen saturation (SaO_2)

An illumination device was designed containing two sets of LEDs emitting specific wavelengths absorbed at different rates by oxygenated and deoxygenated hemoglobin. This was done in line with current pulse oximetry technologies. To produce signals usable in RoR calculations the subject must be illuminated by two wavelengths independently. These wavelengths must be absorbed at different rates by the two components of blood that correspond to SaO_2 ratios, thus demonstrating change in absorbance during pulsatile flow. The wavelengths chosen fall on either side of the 800nm isosbestic point (8). Hb and HbO_2 absorb 800nm at the same rate so 660nm and 910nm emitting LEDs illuminated the subject. The source must be capable of illuminating a subject with a controlled dose of light and precisely controlling that light at two at different frequencies appropriate for measuring blood oxygen saturation

A printed circuit board (PCB) containing a ring of 12 alternating 660nm and 910nm LEDs around an opening in the board for the camera lens to fit inside was designed in EAGLE (AutoDesk, Inc.). The board was designed as a ring to place LEDs equidistant from the lens (Fig. 1).

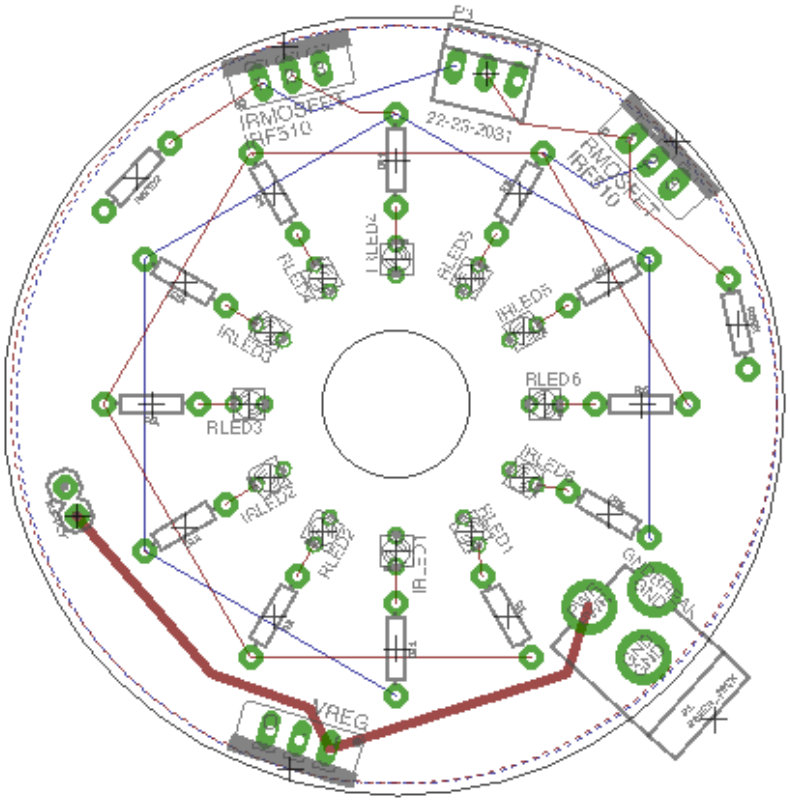

Fig. 1 Board Layout Design for Illumination Source. The ring illumination source was designed in EAGLE with an inner ring placement 12 LEDs. A hole was present in the middle of the board to place the camera lens through. Multiple areas were designated for the connection of power sources with ports facing away from the center of the board.

This provided controlled, homogenous intensities of two wavelengths of light to the subject in view of the lens.

Two N-channel MOSFETS were used to drive the LEDs to the board's ground plane to control the two groups of LEDs independently. The board is powered through a 3.3V low dropout positive voltage regulator with multiple testing points in the board (Fig. 2).

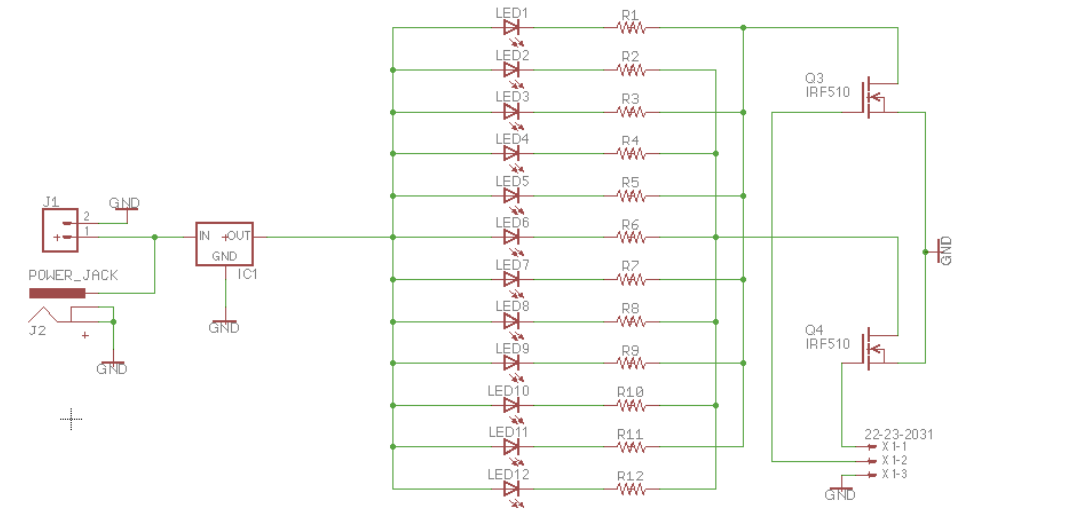

Fig. 2. Schematic Design for Illumination Source. The 12 LEDs were powered by a DC power supply through a voltage regulator. The LEDs were connected in alternating patterns to 2 MOSFETs through resistors. The MOSFETs connected the resistors to ground when receiving a high voltage at its gate.

A Raspberry Pi (RPi) was used to actuate the illumination source. For ease of maintenance control software was written in Python, since it can be written in a standard editor and run from the command line of most computers [5]. The RPi sets the gates of the two MOSFETS high or low, turning the groups of LEDs on and off through the general-purpose input-output (GPIO) pins. To test the designed illumination source the gate of the MOSFET controlling the 660nm LEDs was connected to GPIO pin 17 on the RPi and the MOSFET controlling the 910nm LEDS to pin 23. The board was powered with the Pi's 0V and 5V supply. By supplying the pins with high and low commands alternatingly, the source was illuminated for ~1s with isolated 660nm light and 910nm light switching at a 30Hz frequency (Appendix A).

The setup allows for triggering of the two groups of LEDs independently at high frequencies. The system must capture absorption data at these two wavelengths over time to build two pulse curves based on changes in the individual wavelength absorption.

3.1.2 Design and construct a low-cost, portable imaging system capable of capturing the required data to calculate superficial blood oxygenation

A near-infrared (NIR) camera attachment was used in conjunction with the RPi to acquire a high frequency frame rate video. This inexpensive hardware was selected because a relatively low-cost setup was desired. Acknowledging Nyquist frequencies, to acquire data suitable for desired blood oxygen calculations the sampling rate should be at least twice the frequency of the pulsatile signal [6]. Assuming a maximum pulse frequency of 5Hz (300bpm), data for each of the two wavelengths should be collected at >10Hz resulting in a total system requirement of >20Hz. The system was designed to conservatively sample at 30Hz requiring image capture at 30 frames per second (fps).

A video stream was initialized with the desired resolution of 640x480p. Specific frames from the video stream were then inserted into a buffer to reduce time delays introduced by RPi image writing commands. The saved images must be evenly spaced apart to ascertain pulsatile information. To test the portable imaging system, the saved frames were labeled by the time at which they were captured with 1ms precision (Appendix B).

Images of the human forearm were acquired at distances of 10-100 cm in 10 cm intervals to determine the ideal spatial position of the imaging system relative to the subject. A TOF sensor, the VL53L0X [7], was used to measure the distance from the subject to the camera lens. The TOF sensor chosen has a functional range from 5-120 cm with a distance resolution down to 1 mm [7]. This TOF system was implemented with the camera set up to label each acquired frame with the distance at which the image was taken. This was used to ensure that the distance between the subject and camera remained constant over the image acquisition period, as changes in this dimension would alter the measured absorbance of light. Because the system is optically based, the measured absorption of light by the subject is related to the distance that the light travels. This

system was designed to produce signals from which a ratio of absorbance could be measured. In calibrating the output R-value, distance plays a large role. The TOF sensor allows for data collection at a predetermined optimal distance. Any images acquired at other distances require further calibration and research.

3.1.3 Trigger image acquisition with wavelength illumination

To acquire data about the subject at the two required wavelengths, image capture was synchronized with the illumination source LED activation. The two data sets were collected independently, as having both LEDs turned on would alter the absorption rates of the blood. This was done by altering between the two sets of LEDs and synchronizing the save function of adjacent frames from the video stream. All images captured during the activation of wavelength A and B were saved in two different folders.

The system was designed to follow these steps to acquire the data required for superficial blood oxygen calculations:

1. Enable LEDs with 660nm wavelength
2. Capture image (at 660nm)
3. Save (in 660nm folder)
4. Disable LEDS with 660nm wavelength
5. Enable LEDs with 910nm wavelength
6. Capture image (at 910nm)
7. Save (in 910nm folder)
8. Disable LEDs with 910nm wavelength
9. Repeat steps 1-9

This loop repeated for the duration of the imaging. A small time delay was added between each step to ensure that the images were captured when one group of LEDs was on and not during the triggering of the alternate group of LEDs.

The system output two folders of 15 images, allowing analysis of changes in the subject's light absorption over 1 second for two independent wavelengths (Appendix C). The system used the assumption that the time elapsed between the first image captured at 660nm and the first image captured at 910nm was small enough to analyze the data points from the two folders as though they were acquired simultaneously.

Images were acquired at two non-isosbestic wavelengths at a high enough frequency to resolve pulsatile information. The synchronization system was tested by removing the connection to the MOSFET controlling the LEDs at 910nm. This decision temporarily turned one group of LEDs off and allowed the other group to turn on and off. Data was acquired over 1s with the synchronized illumination source facing the lens of the imaging system and analyzed the two saved folders of images. All 15 images contained in the 660nm folder should show an illuminated ring of light. The 15 images in the 910nm folder were expected to show no illumination because the LEDs in this group were turned off.

3.2 Data post-processing

3.2.1 Extract a single pixel's time-varying absorption data from one wavelength folder

To extract data about changes in light absorption of the subject, the images required pixel-by-pixel color analysis. Changes in pixel color between images reveal information about the change in light absorption of the area corresponding to that pixel. To perform this computationally heavy pixel analysis, the images, saved in an 8-bit RAW format, were loaded

and analyzed in MATLAB (The MathWorks). To separately analyze data produced by the 660nm and 910nm exposure, the folders of acquired images were imported separately.

The imaging system was limited by its optimal 640x480 resolution video capturing capabilities. The high frame rate prevented increased resolution, thus limiting data analysis to images composed of 640x480 pixels. In MATLAB the images were imported as a 640x480 matrix of assigned quantitative values representing the pixel's color information. Each pixel of the colored image was represented as a specific mixture of red, green, and blue values ranging from 0-255 (8-bits).

It was hypothesized that by analyzing a single pixel's RGB values over the full set of images, time-varying changes in the corresponding area's light absorption could be determined. If "image0" corresponds to time=0s and 90 images are acquired at 30fps then "image89" corresponds to time=3s. In Matlab a single pixel specified by x and y coordinates was chosen, and its RGB values were recorded for each image, providing 3 sets of 90 data points over a three second duration (Appendix D). The subject of the images was illuminated by 660nm light. A test pixel was chosen based on its location corresponding to an area on the wrist denoted in literature as having prominent vasculature. Due to superficial vasculature, this area was expected to have blood flowing through it, producing a changing level of absorbance due to fluctuations in HbO_2 and Hb concentrations. The pulsatile flow also changes the pressure of blood pumping through the area, which was expected to alter the amount of light absorbed at that site. By analyzing the quantitative color description of the pixel over time, the system allowed for creation of a pulse curve for the 660nm wavelength. This was then repeated for 910nm exposed images compiled separately. These pulse curves should later be used to determine information necessary for blood oxygen calculations.

3.2.2 Experiment to test changes in absorption of specific wavelength of control vs biological tissue

To demonstrate the role of physiology and potentially blood flow in the time-varying RGB changes, a pixel corresponding to biological tissue was compared to a pixel corresponding to a control. 90 images were acquired over 3 seconds with two subjects illuminated by 660nm. 10 pixels were chosen on the wrist and 10 pixels were chosen corresponding to areas on the table. By acquiring images with the two subjects in view, confounding variables such as changes in illumination intensity or distance from the camera to the subjects were eliminated. The RGB values of the chosen 20 pixels were plotted over the 90 images and the two groups were compared. A median filter with a three-pixel window was applied to a single pixel through time (Appendix E), reducing the effect of rapidly changing signals due to high frequency noise. This experiment aimed to compare changes in absorption of a biological system to changes of absorption of a fixed rate-of absorption subject. The goal was to show that any changes detected were not caused by variances in the light source or flaws in the image capture method.

3.2.3 Multi-pixel analysis and mapping of changes in absorption values over time

After demonstrating the system's ability to measure changes in absorption of a single pixel over time, the system was tested using multi-pixel analysis. Vasculature has blood flowing through it, which experiences changes in its composition of oxygenated and deoxygenated hemoglobin. As previously discussed, the rate of absorption of the emitting wavelengths chosen for this device depends on the changing composition of the blood. The areas with underlying vasculature contained in the image should correspond with pixels demonstrating larger changes

over time. It was hypothesized that the system could create a perfusion map highlighting vasculature with substantial blood flow.

The previous single-pixel analysis was applied over the entire image. Each pixel in the 640x480 matrix had its RGB-values recorded over n images (n=90 and n=300 were used in this study). The total change in absorbance over the sampling time was calculated by subtracting the minimum RGB-value from the maximum. To reduce the confounding effect of large changes in absorbance occurring for reasons other than changes in blood composition, the calculation was performed by subtracting the average of the bottom 10% of the data points from the average of the top 10% of data points for each pixel. The system then rewrote the image matrix with the change value of each pixel over time. The difference matrix was then converted to intensity values from 0 to 1 allowing it to be written as a gray-scale image mask representing locations where absorption differences were observed (Appendix F). The individual pixels showing the largest change in RGB-values correspond to black pixels in the output map image and the pixels showing the smallest change correspond to white pixels.

This was tested by capturing a series of images of a stationary arm and a stationary background exposed to either 910nm or 660nm light over a three second duration.

3.2.4 Ascertain pulsatile information from images

Based on the assumption that the changes in RGB-values are directly related to changes in absorption of the specific illumination wavelength, a single-pixel analysis of an area corresponding to vasculature should produce a pulsatile signal. Using the perfusion map created a pixel with known change in absorption (dark on the map) was chosen and analyzed over time. Fast Fourier Transforms were applied in MATLAB on the selected source signal to ascertain the

power spectrum (Appendix G). The power of frequency components contained within the range of 0-2Hz were analyzed to determine if heart rate/pulse could be extrapolated by the system. The frequency range of 0-2Hz was used because many biological signals targeted by this system occur within this range. The average heart rate ranges from 50bpm to 120bpm [9]. This information was used to create an operational frequency band of 0.8-2Hz. The pulse frequency was designated as the frequency that corresponded to the highest power within this operational frequency.

To test this, 300 images were taken over 10s at a distance of 30cm with the subject illuminated by 910nm emitting LEDs. Two 2x2 pixel areas of interest were chosen based on the perfusion map. Both areas were colored black on the perfusion map, indicating a large change in absorption over time. One area was chosen on visible vasculature, where change in absorption was expected, and another area was chosen at the edge between the arm and the table, where large change in absorption was not expected.

4 Results

4.1 Synchronous high frequency illuminated image acquisition

4.1.1 Design a synchronous LED source appropriate for measuring blood oxygen saturation (SaO_2)

An oscilloscope with connections to the GPIO pins 17 and 23 was used to determine the high frequency altering LED activation. These pins were connected to the two MOSFETs controlling the groups of LEDs. The MOSFET controlling the ring of 660nm LEDs received 3.3V simultaneously with the MOSFET controlling the 910nm LEDs receiving 0V (Fig 3).

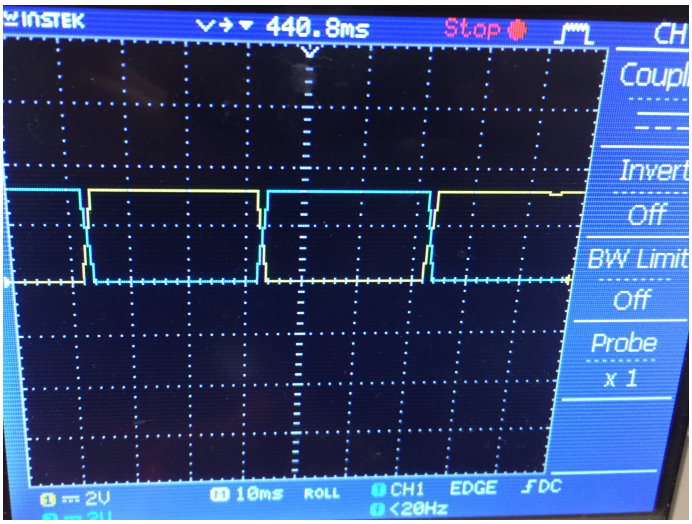

Fig. 3. Oscilloscope Voltage of GPIO Pins. The voltages at GPIO pins 17 and 23 were measured. They demonstrated an alternating high and low voltage indicating that when one MOSFET was receiving a 5V supply the other MOSFET was receiving a 0V supply.

The signal alternated at 30Hz over a 1 second duration (Fig. 4).

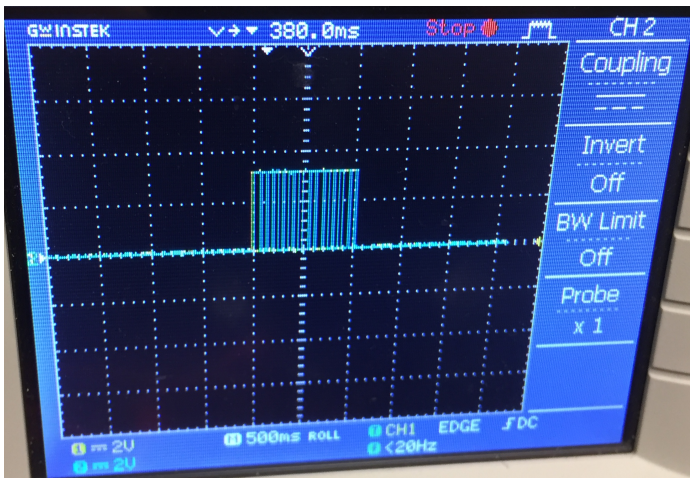

Fig. 4. Oscilloscope Voltage of GPIO Pins Over Duration of System Output. The pattern previously described was continued for a 1s duration

4.1.2 Design and construct a low-cost, portable imaging system capable of capturing the required data to calculate superficial blood oxygenation

It was hypothesized that images could be acquired at regular intervals to adequately analyze pulse curves. Over 10 seconds of image acquisition at 30fps the average time elapsed between each saved frame was 33ms with <5% error. The test was inherently flawed due to its limitation to 1ms precision in the Raspberry Pi's time label function.

The optimal resolution of the images was determined to consistently be 640x480 at frame rates >30fps. The optimal distance between the camera lens and the subject was determined to be 10-30 cm under natural lighting.

4.1.3 Trigger image acquisition with wavelength illumination

Testing the system synchronization the voltages applied to the MOSFETs from the GPIO pins were analyzed. The LEDs were being turned on/off at 30Hz with a small time delay to ensure that only one set of LEDs was activated at the time of image capture (Fig. 5).

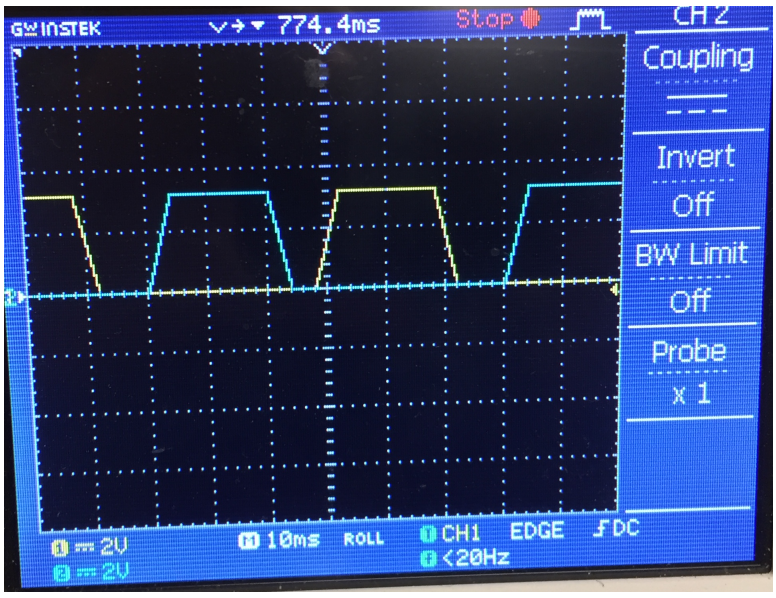

Fig. 5. Oscilloscope Output of GPIO Pins with Added Time Delay. The voltages at GPIO pins 17 and 23 were measured. They demonstrated an alternating high and low voltage

indicating that when one MOSFET was receiving a 5V supply the other MOSFET was receiving a 0V supply. A time delay was added between triggering to turn both MOSFETs off before turning the desired one on.

The results of the experiment used to test the synchronization of the system contradicted what was expected. 9 of the 15 images taken under supposedly no illumination (because the 910nm emitting LEDs were turned off) appeared dark but 6 images showed the LEDs emitting 660nm in the process of turning on (Fig. 6). 10 of the images contained in the 660nm folder displayed the LEDs in an "on" state, but they were varying intensities. 5 images appeared dark (Fig. 7). Some of the saved images were captured while the wrong LEDs were turning on or off and not during their intended time frame.

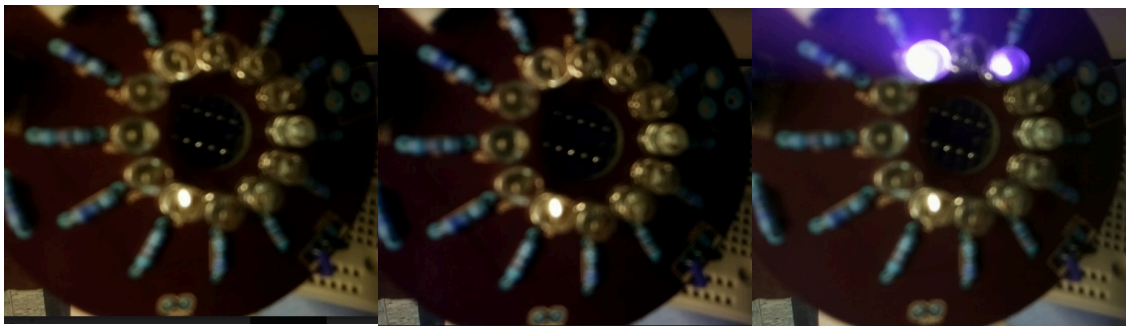

Fig. 6. Images of Light Source Taken from "Off" Folder. The LEDs were disconnected from the board's ground plane so they should be "off" during the capturing of these images.

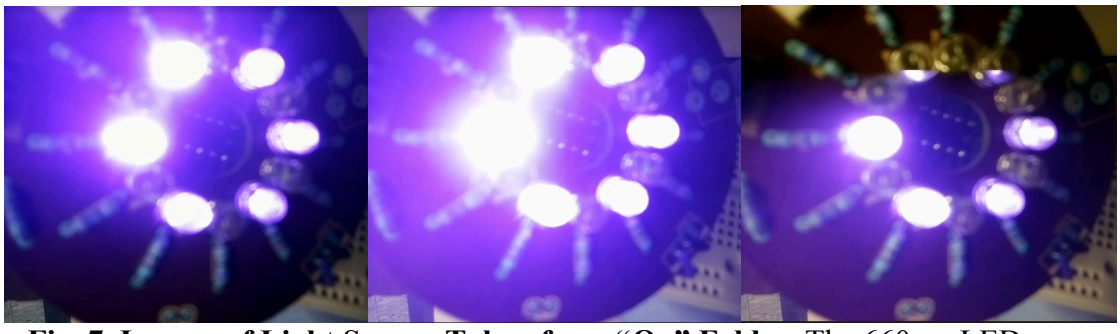

Fig. 7. Images of Light Source Taken from "On" Folder. The 660nm LEDs were supposedly connected to the ground plane during the capturing of these images. In some of the images the group of LEDs is emitting light as expected. Other images show only some of the LEDs in the group emitting light.

4.2 Data post-processing

4.2.1 Extract a single pixel's time-varying absorption data from one wavelength folder

To determine time-varying changes in the chosen area's absorption of a specific wavelength (660nm) the corresponding pixel's raw RGB values were graphed over 90 images (3s) (Fig. 8).

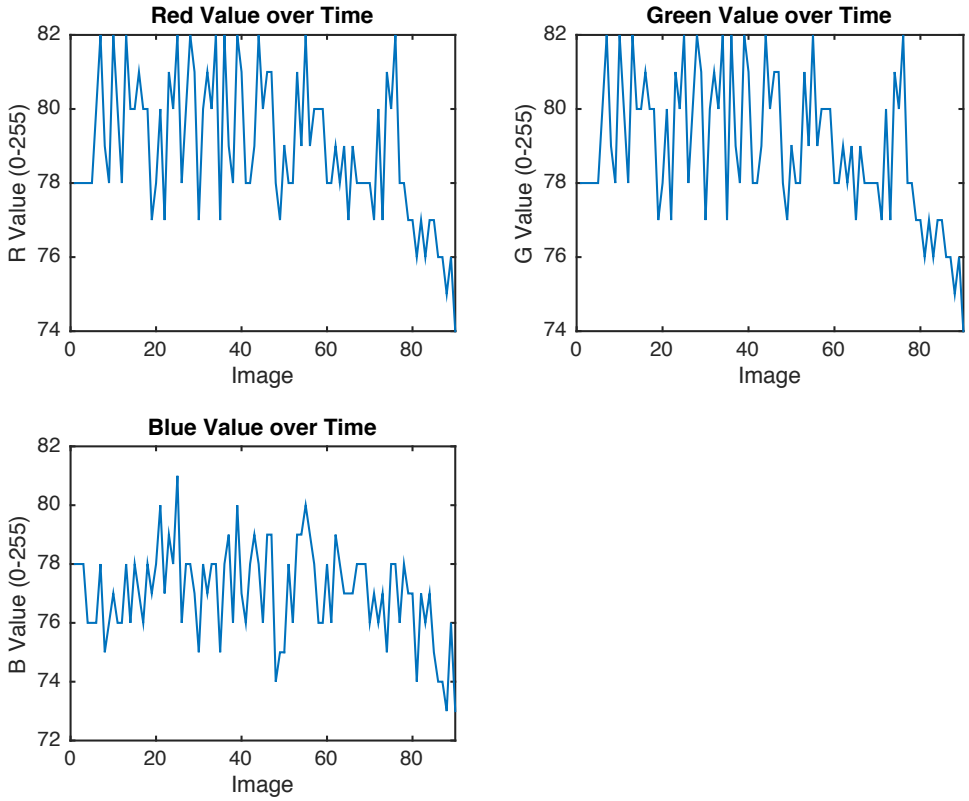

Fig. 8. Graphs of the RGB Values of a Single Pixel over 90 Images Taken at 30fps. The R-value of the chosen single pixel ranged from 74-82 with a mean value of 78.7. The G-value of the chosen single pixel ranged from 74-82 with a mean value of 78.5. The B-value of a single pixel ranged from 73-81 with a mean value of 76.8.

This data demonstrates time-varying changes in RGB values captured by the system. The images acquired of vasculature were expected to show period absorbance at a constant wavelength due to absorption of HbO_2. and Hb.

4.2.2 Experiment to test changes in absorption of specific wavelength of biological tissue versus control

The changes in RGB values between the pixels in each group (wrist and control) were compared. The data is summarized by a single pixel chosen from each group (Fig. 9) with absorption for the wrist area ranging from 73-82 over three seconds and absorption for the blank background ranging from 16-19. The average range of absorbance in the chosen experimental pixels was 10.2 while the average range in the control pixels was 2.7. By comparing the experimental and control group, the data supports the system's capability in measuring changes in absorption of biological tissue relative to a background with a fixed rate of absorption.

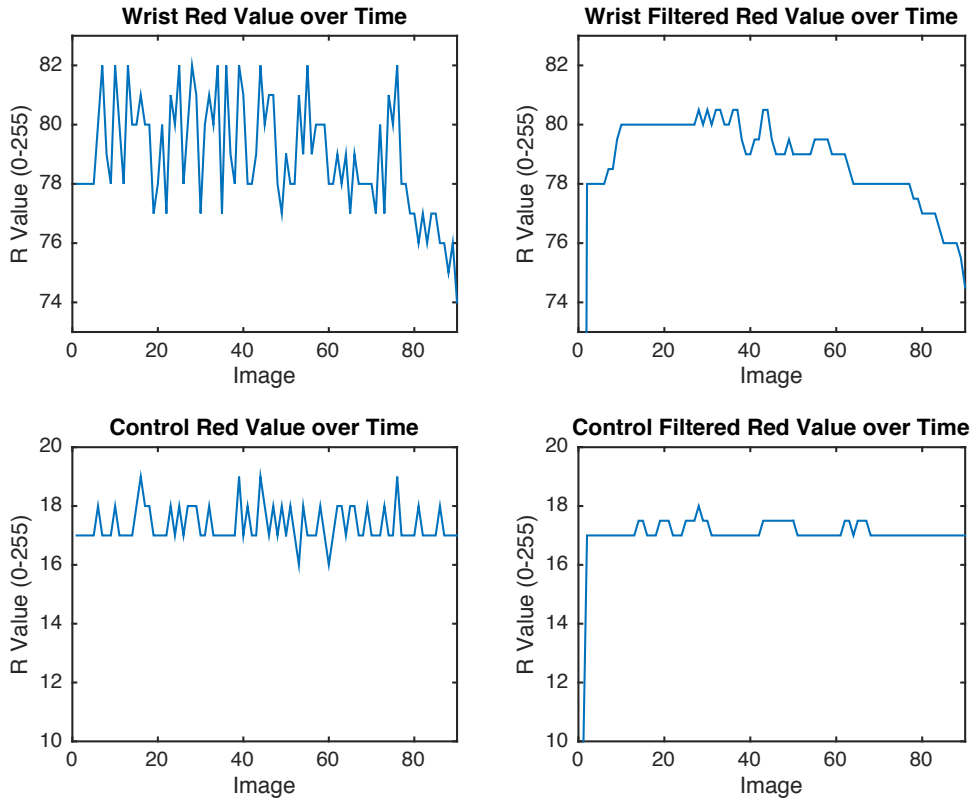

Fig. 9. Graphs of the R-Values of a Single Pixel chosen from Wrist and Control. The wrist pixel represents an area of vasculature. When filtered through median filter with a three-

pixel window a decrease from 81 to 74 in R-value is seen. The control pixel, a pixel chosen in the background of the image, represents an area of constant absorbance rates. The filtered R-value ranges from 17-18.

A two-sample t-test was conducted to determine if the average change in absorbance over 3s of the vascular pixels was statistically different than the average change of the background pixels. Ten pixels were sampled for each group and the t-test was performed in JMP with a p-value of 0.042.

4.2.3 Multi-pixel analysis and mapping of changes in absorption values over time

The perfusion maps of the arm were expected to display highlighted areas of vasculature while the perfusion amps of the solid background were expected to show no highlighted areas. Under the 660 nm emitted LEDs the perfusion map of the wrist shows darkened areas (Fig. 10ab) that follow the expected vasculature pattern.

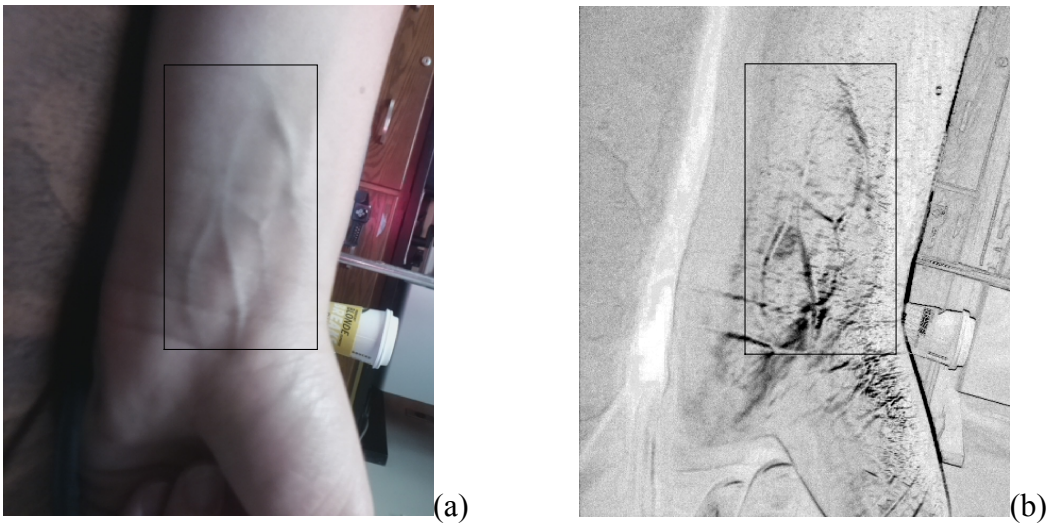

(a) (b)

Fig. 10. Wrist Under 660nm exposure. The distance between the subject and camera lens was 10cm and the illumination ring was emitting 660nm light. A black rectangular box corresponds to an area of vasculature as seen in the sample colored image (a). A perfusion map (b) was created from 90 images acquired over 3s. The dark areas of the map correspond to areas with the greatest change in RGB values over the image capture duration.

The map of the solid background appears to have the same absorption across the whole image (Fig. 11ab). In both images the edges of objects in the images are darkened. This was likely due to slight camera movement causing large changes in RGB-values between frames. Because the maps are created by comparing the changes in values, slight movement buries clear illustration of the much smaller changes due to blood flow.

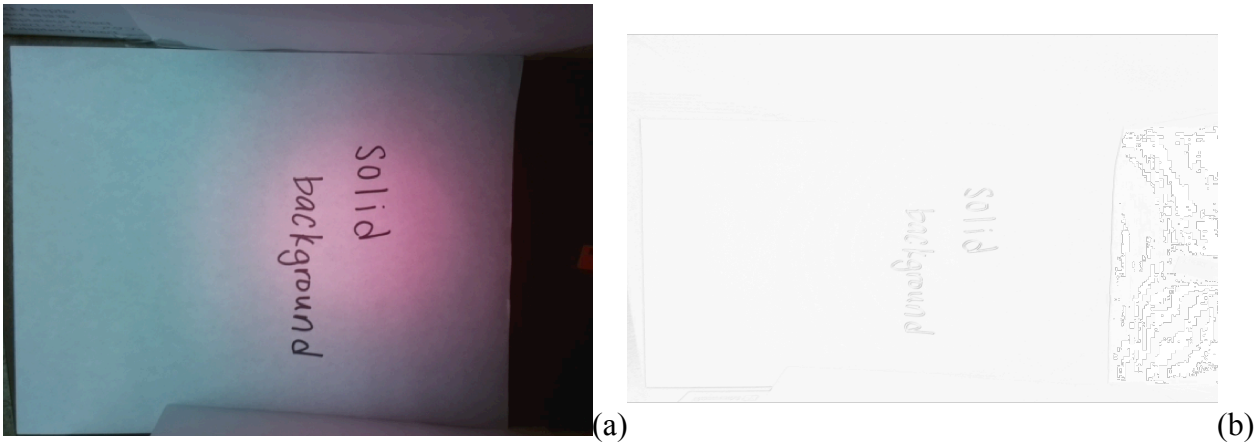

(a) (b)

Fig. 11. Background Under 660nm exposure. The distance between the subject and camera lens was 20cm and the illumination ring was emitting 660nm light. 90 images similar to the sample image of a piece of paper (a) were acquired over 3s. The background has a constant rate of absorption of light so minimal change in RGB values was expected in the perfusion map (b).

Striations can be seen under 910nm LED illumination (Fig. 12,13). This data set was acquired with the light source 20cm from the subject. Although vasculature in the distal forearm is highlighted the central forearm area and the noticeable striations indicate that the light source is blowing out the image and creating light artifacts. The optimal distance from the subject to the light source and the camera lens was determined to be 30cm. The results provide proof of concept that the system can create a map highlighting the areas of greatest changes in absorption of a

specific wavelength therefore visualizing perfusion. This analysis highlighted vasculature superficial to the dermal tissue and provided information on blood flow in the focus area.

Fig. 12. Sample Colored Image of Forearm Under 910nm exposure. The distance between the subject and camera lens was 20cm and the illumination ring was emitting 910nm light.

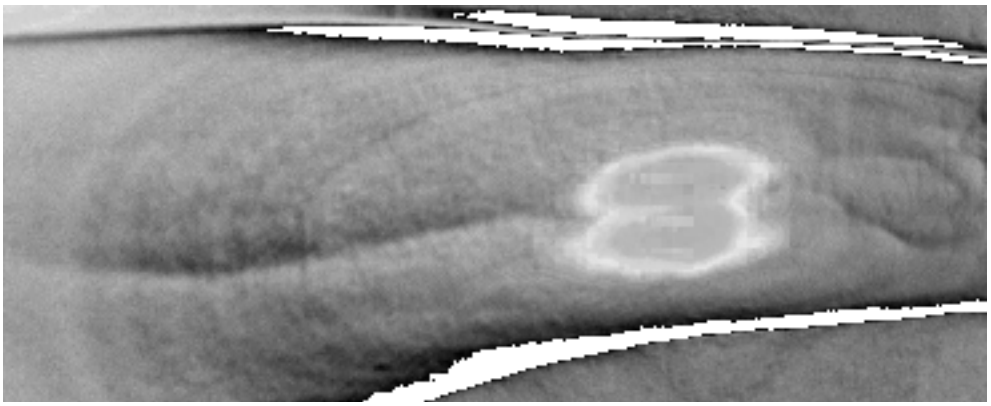

Fig. 13. Output Perfusion Map of Forearm Under 910nm exposure. 90 images were acquired over 3s. The dark areas of the map correspond to areas with the greatest change in RGB values over the image capture duration. A small area in the middle shows light undefined space likely caused by the 910nm light source blowing out that area.

Explain striations

4.2.4 Ascertain pulsatile information from images

It was hypothesized that the FFT spectrum graphs of the pixels chosen in the area between the table and the arm would not exhibit high power of frequencies in the 0.8-2Hz spectrum. The four pixels, although adjacent, demonstrated differing results but the dominant frequencies within

the operational frequency band had a maximum power of 0.05 (Fig. 14). The high power at low frequencies (<0.1Hz) is explained by a DC offset in the signal that has a frequency of 0. This low-frequency information is not helpful in determining pulsatile information so it will be ignored for data analysis.

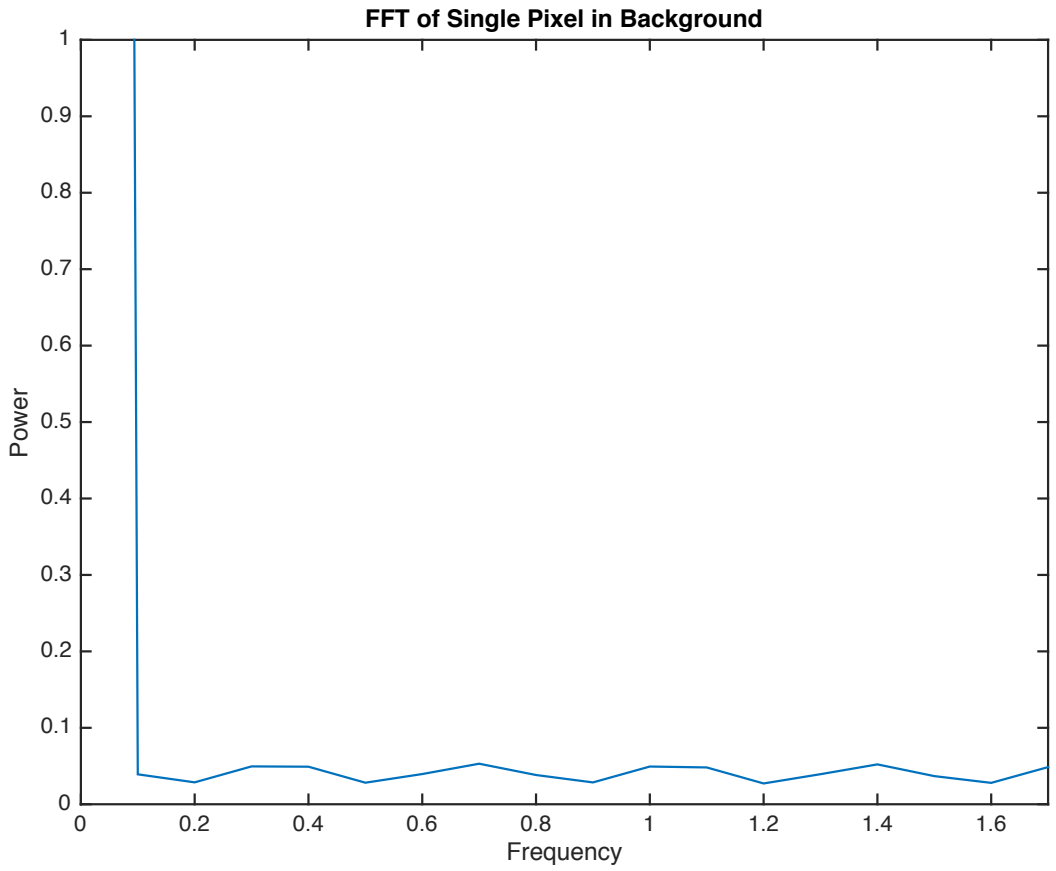

Fig. 14. Graph of FFT Calculations Performed on Single Pixel over Area Between Arm and Table. The pixel corresponded to a darkened area on the perfusion map. The frequencies within the operational band are marked by low powers (<0.05) for this pixel.

This supports the belief that the changes in absorption in this area were likely caused by aperiodic movement. The FFT information from the pixels corresponding to existing vasculature contained frequencies within the analyzed range with a maximum power of 0.55. Frequencies of 0, 0.4, 0.7, and 1 Hz were determined to be the dominant frequencies from a single pixel located in the

vasculature (Fig. 15), but analyzing the other pixels over existing vasculature produces differing powers of frequencies across the selected spectrum.

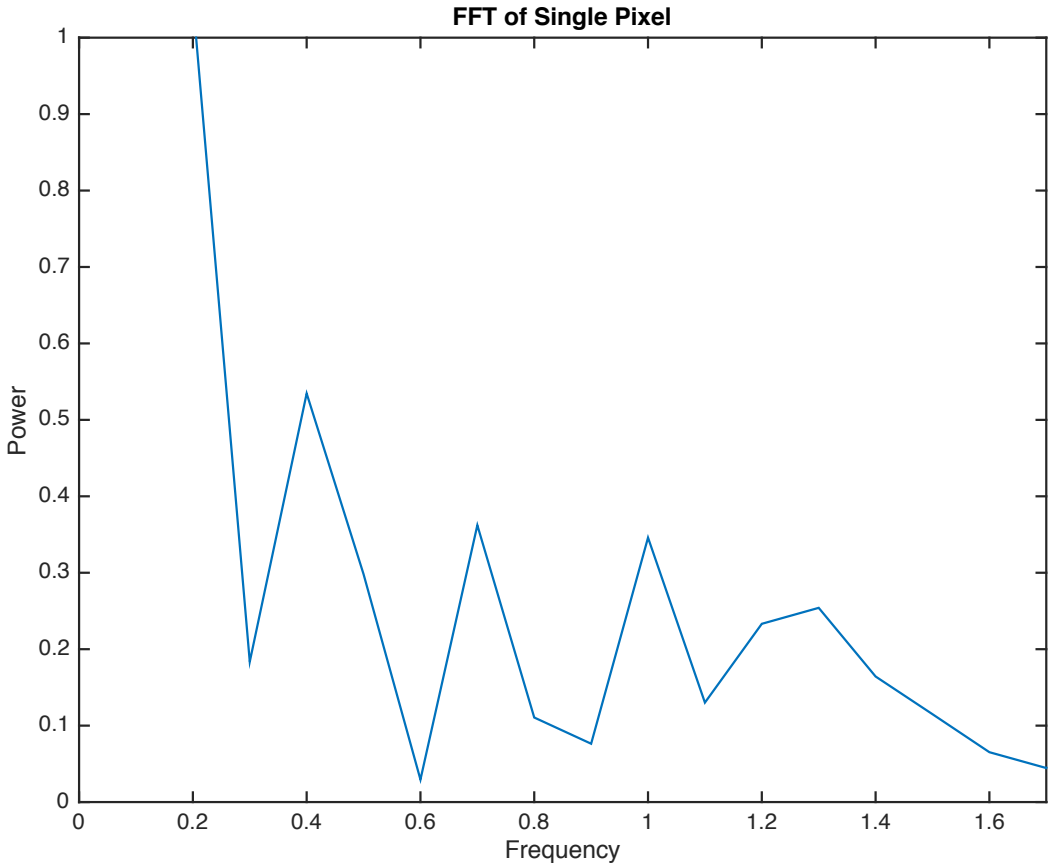

Fig. 15. Graph of FFT Calculations Performed on Single Pixel over Vascular Area. The pixel corresponded to a darkened area on the perfusion map.

The heart rate measured from one selected pixel corresponding to a vein in the forearm was 60bpm (1Hz). Each of the "vascular" pixels chosen showed >0.5 power at 0.4Hz. It is possible that the 0.4Hz component of the signal was due to respiration but it was not studied in this experiment. Overall the powers of frequencies determined by the FFTs were all low (<1) indicating no identifiable frequency dominating the signal.

5 Discussion

The first aim of this project proposed to design and construct an optically based system capable of obtaining the data required to calculate superficial blood oxygenation and perfusion without direct contact with dermal tissue. Testing the designed light source demonstrated the system's ability to illuminate biological tissue independently with two wavelengths (Fig. 3) that have differing rates of absorption depending on oxygenated and deoxygenated hemoglobin ratios. To acquire data useful in calculating blood oxygenation, the absorption changes of the biological tissue was sampled at a high enough frequency to measure pulsatile information. Falling in line with traditional pulse oximeter technology the collected absorption data was obtained from a distance under a single wavelength. The system can detect two independent wavelength absorption signals that can be used in RoR calculations to determine SpO_2 levels.

When testing the system it was demonstrated that the high frequency image acquisition produced images at normal intervals and with sufficient resolution to analyze changes in absorbance of light by the subject over time. Equally timed images captured at 30Hz provided matrices of discrete data that could be analyzed over time providing time-varying absorbance information. The synchronization of the image acquisition with the illumination was required to compile simultaneous pulse curves of biological tissue under two isolated wavelengths. The outcome of this experiment demonstrated that the imaging system had limitations in its internal timing mechanism causing irregular image acquisition (Fig. 6,7). The disagreement between the saved frames in each folder was likely caused by the RPi's internal delay in saving frames from a captured video stream. The LEDs were triggered correctly but the frames that the system chose to save were delayed and did not correspond to the specified wavelength. The exposure and

saving methods were altered in an attempt to overcome this obstacle but the internal mechanisms of pulling frames from a video stream prevented isolated data capture. Following these results, the system was limited to focusing on acquisition and analysis of images illuminated by a single wavelength at a time. This limits the system's ability to output a ratio required for blood oxygen measurements and calibration but does not hinder the proof of concept. Future work can be done to pull and write specific frames *after* video has been captured and saved, but it will be difficult to consistently determine which frames correspond to which wavelength retroactively. There will also be difficulty in ensuring that saved frames occurred during the peak LED emitting period and not during its activation period.

The second aim of the project was to use the data acquired by the system to determine biological signals. Single pixel RGB analysis of biological tissue indicated changing absorbance over time. The changes had equivalent ranges in the red, green, and blue values (Fig. 8) so no specific color value was determined to be superior in determining absorbance changes. The data did not exhibit identifiable periodic absorbance curves. Over the three second period it was expected that 2-6 pulse spikes would be measured (assuming a HR of 40-120bpm). The data did not exhibit clearly distinguishable pulse curves so the system was tested to determine if the measured biological tissue's changes in absorbance were different compared to a constant rate of absorption background. A p-value of 0.042 was found indicating that the changes in biological tissue absorption (Fig. 9) were statistically different than the changes in a constant rate of absorption background (alpha value of 0.05). These results support the claim that changes detected are likely related to a physiological characteristic or signal but the small sample size of 10 pixels limits this conclusion. ANOVA should be completed over every pixel in the image with the three pixel groups being areas of vasculature, tissue without superficial vasculature, and

background. The possibility of completing this is questioned because it is difficult to determine exactly which pixels correspond to each group over the whole image and any slight movement of tissue or blood vessel (which is natural with pulse) would confound the analysis.

The lack of measurable pulse curves limited the system's ability to produce measurements usable in blood oxygen saturation calculations. The system aimed to map areas of blood flow by highlighting the areas that demonstrated the largest change in absorption over time when exposed to a constant wavelength. Vasculature was highlighted as expected, but edges between surfaces were also highlighted (Fig. 10,11). This indicates that those edges experience a large change in absorbance over time, which can be explained by movement of the camera lens or subject. Light artifacts might be removed by reducing the intensity of light emitted by the illumination source but this might reduce the detectable change in absorption. The appearance of motion and light artifact in the mapping images might be reduced by implementing a 2D median filter over the output image but some foreseen challenges include degradation of changes detected in the blood vessels themselves. This would result in an illumination of general areas of blood flow (i.e. the forearm) but the vessels themselves would not be distinguishable.

Determining single pixel's spectral Fourier frequencies over time reveals dominant frequencies contributing to time-varying absorbance signals. FFT graphs of vascular pixels shows higher power frequency components in the operational frequency band than background pixels (Fig. 14,15). For all pixels the powers in the target range for pulse rate were very low (<1) indicating that the technique may not measure pulse rate accurately or that there might not be enough samples in the signal to pull pulsatile information. Heart rate changes with respiration, which might change the periodicity of absorption over the three-second data acquisition period. 1,800 images providing one minute of absorption values for a single pixel might improve the

powers of frequencies within this range but this would be computationally difficult to perform. It would also be difficult to maintain a constant heart rate over that length of time and the physiological measurements would not be practical or real-time. The highest power frequency in the operational heart rate band was recorded as 1Hz in some vascular pixels and 1.2Hz in other pixels. Because of the variability in the frequency powers over different areas of vasculature it is unlikely that this technique can be used to accurately determine pulse rate.

6 Conclusion

The work completed provides promising preliminary data for future research into non-contact blood perfusion and pulse-oximetry technology. The perfusion mapping technique needs to be adapted to refresh with new data over time thus providing real-time perfusion video. This system needs to be tested over other areas of the body to determine if it is limited to forearm measurements. Because the source is illuminated with light that is absorbed and scattered by biological tissue it needs to be determined what effect the thickness and coloration of skin has on the data produced by the system. With hopes to calibrate calculations performed by this system to blood oxygen saturation distance between the system and the subject must be accounted for. This can only be done once the synchronized capture issues with this system are resolved to create simultaneous pulse curves.

The thesis work produced a system capable of illuminating a subject with wavelength required in blood oxygen calculations and acquiring high frequency data containing absorbance changes over time. The work successfully illustrated blood flow through superficial vasculature. The systems functional imaging depth was not measured but should be researched to determine how much information the system can provide about sub-dermal perfusion or perfusion in areas of high fatty concentrations.

The perfusion mapping could be used to determine if dermal wounds and their surrounding areas are receiving sufficient blood supply and for noninvasive vein detection. This device aims to ultimately allow for blood oxygen saturation measurements to be made non-invasively from a distance, which is especially useful in burn patients, isolating them from the high risk of infection introduced with any dermal contact.

References

1. Schreml, S., Szeimies, R., Prantl, L., Karrer, S., Landthaler, M., & Babilas, P. (2010, April 15). Oxygen in acute and chronic wound healing. Retrieved July 20, 2017, from http://onlinelibrary.wiley.com/doi/10.1111/j.1365-2133.2010.09804.x/full
2. Mardirossian, G., & Schneider, R. E. (1992). Limitations of pulse oximetry. Retrieved July 20, 2017, from https://www.ncbi.nlm.nih.gov/pmc/articles/PMC2148612/?page=3
3. Tremper, K. K., & Barker, S. J. (1989). Pulse Oximetry. *Anesthesiology,70*(1), 98-108. doi:10.1097/00000542-198901000-00019
4. Aoyagi, T. (2003). Pulse oximetry: its invention, theory, and future. *Journal of Anesthesia,17*(4), 259-266. doi:10.1007/s00540-003-0192-6
5. Python. (n.d.). Retrieved July 20, 2017, from https://www.raspberrypi.org/documentation/usage/python/
6. Nyquist Frequency. (n.d.). Retrieved July 20, 2017, from http://mathworld.wolfram.com/NyquistFrequency.html
7. Industries, A. (n.d.). Adafruit VL53L0X Time of Flight Distance Sensor - ~30 to 1000mm. Retrieved July 20, 2017, from https://www.adafruit.com/product/3317
8. Pulse Oximetry. : International Anesthesiology Clinics. (n.d.). Retrieved July 20, 2017, from http://journals.lww.com/anesthesiaclinics/Citation/1987/02540/Pulse_Oximetry.9.aspx
9. Center for Devices and Radiological Health. (n.d.). Premarket Notification 510(k). Retrieved July 20, 2017, from https://www.fda.gov/medicaldevices/deviceregulationandguidance/howtomarketyourdevice/premarketsubmissions/premarketnotification510k/

Appendix

Appendix A. Python Code for Triggering Illumination Source at 30Hz.

```
import RPi.GPIO as GPIO
import time
from time import sleep
import io

GPIO.setwarnings(False)
GPIO.setmode(GPIO.BCM)
GPIO.setup(23, GPIO.OUT)
GPIO.setup(17, GPIO.OUT)
chan_list = (23,17)

GPIO.output(chan_list, GPIO.LOW)

time.sleep(2)
for i in range(30):

    if i%2==0:
        GPIO.output(chan_list, (GPIO.HIGH,GPIO.LOW))
        time.sleep(0.03)

    else:
        GPIO.output(chan_list, (GPIO.LOW,GPIO.HIGH))
        time.sleep(0.03)

GPIO.output(chan_list, GPIO.LOW)
time.sleep(1)
```

Appendix B. Python Code for Acquiring Images with 640x480 resolution at 30fps. Each image was labeled by the time at which it was captured with 1ms resolution.

```
import io
import time
import picamera
from datetime import datetime

with picamera.PiCamera() as camera:
    # Set the camera's resolution to VGA @30fps and give it a couple
    # of seconds to measure exposure etc.
    camera.resolution = (640, 480)
    camera.framerate = 30
```

```
    time.sleep(3)
    # Set up i in-memory streams
    outputs = [io.BytesIO() for i in range(30)]
    start = time.time()
    camera.capture_sequence([
       'image%s.jpg' % str(datetime.now(),strftime('%H:%M:%S:%f'))
       for i in range(30)
       ],use_video_port=True)
        finish = time.time()
```

Appendix C. Python Code for Synchronizing Image Acquisition and Light Source Triggering. The images were saved in folders depending on which light source was turned on at the time of its capture.

```
import sys
sys.path.append('/usr/local/lib/python3.4/site-packages')
import cv2
import numpy

from PyQt5 import QtCore, QtGui, QtWidgets
import imutils
import argparse
from imutils.video import VideoStream
import qimage2ndarray

import RPi.GPIO as GPIO
import time
from time import sleep
import io
import picamera
from datetime import datetime

GPIO.setwarnings(False)
GPIO.setmode(GPIO.BCM)
GPIO.setup(23, GPIO.OUT)
GPIO.setup(17, GPIO.OUT)
chan_list = (23,17)

GPIO.output(chan_list, GPIO.LOW)
ap = argparse.ArgumentParser()
ap.add_argument("-p","--picamera", type=int, default=1,
            help="Pi camera default")
args = vars(ap.parse_args())
vs = VideoStream(usePiCamera=args["picamera"]>0).start()
```

```
capture = vs

time.sleep(2)
for i in range(30):
##    frame = capture.read()
##    cv2.imwrite('wavelengthA%02d.jpg' % i, frame)
##    time.sleep(0.05)

   if i%2==0:
      GPIO.output(chan_list, (GPIO.LOW,GPIO.LOW))
      time.sleep(0.01)
      GPIO.output(chan_list, (GPIO.HIGH,GPIO.LOW))
      time.sleep(0.01)
      frame = capture.read()
      cv2.imwrite('wavelengthA%02d.jpg' % i, frame)
      time.sleep(0.01)

   else:
      GPIO.output(chan_list, (GPIO.LOW,GPIO.LOW))
      time.sleep(0.01)
      GPIO.output(chan_list, (GPIO.LOW,GPIO.HIGH))
      time.sleep(0.01)
      frame = capture.read()
      cv2.imwrite('wavelengthB%02d.jpg' % i, frame)
      time.sleep(0.01)


GPIO.output(chan_list, GPIO.LOW)
time.sleep(1)
```

Appendix D. MATLAB code of Analyzing RGB values of a Single Pixel over Time.

```
n=90;

r=zeros(480,640,n);
g=zeros(480,640,n);
b=zeros(480,640,n);

for k = 1:n

   jpgFileName = strcat('image', num2str(k-1), '.jpg');
   imageData = imread(jpgFileName);
   rValue = imageData(1:480, 1:640, 1);
   r(:,:,k)=rValue;

end
```

```
for k = 1:n

    jpgFileName = strcat('image', num2str(k-1), '.jpg');
    imageData = imread(jpgFileName);
    gValue = imageData(1:480, 1:640, 2);
    g(:,:,k)=gValue;

end
for k = 1:n

    jpgFileName = strcat('image', num2str(k-1), '.jpg');
    imageData = imread(jpgFileName);
    bValue = imageData(1:480, 1:640, 3);
    b(:,:,k)=bValue;

end

x=170;
y=260;

subplot(2,2,1)
r2=r(y,x,:);
r3=r2(:).';
plot(r3);
title('Red Value over Time')
ylabel('R Value (0-255)')
xlabel('Image')
xlim([0 90])

subplot(2,2,2)
g2=g(y,x,:);
g3=g2(:).';
plot(r3);
title('Green Value over Time')
ylabel('G Value (0-255)')
xlabel('Image')
xlim([0 90])

subplot(2,2,3)
b2=b(y,x,:);
b3=b2(:).';
plot(b3);
title('Blue Value over Time')
ylabel('B Value (0-255)')
xlabel('Image')
xlim([0 90])
```

Appendix E. MATLAB Code of Filtered Single Pixel RGB Values over Time.

```
n=90;

rgb=zeros(480,640,n);

for k = 1:n

   jpgFileName = strcat('image', num2str(k-1), '.jpg');
   imageData = imread(jpgFileName);
   rgbValue = imageData(1:480, 1:640, 1);
   rgb (:,:,k)=rgbValue;

end

x=170;
y=260;
x2=107;
y2=161;

subplot(2,2,1)
rgb2=rgb(y,x,:);
rgb3=rgb2(:).';
plot(rgb3);
title('Wrist Red Value over Time')
ylabel('R Value (0-255)')
xlabel('Image')
xlim([0 90])
ylim([73 83])

subplot(2,2,2)
rgb2=rgb(y,x,:);
rgb3=rgb2(:).';
filt = medfilt1(rgb3,10);
plot(filt);
title('Wrist Filtered Red Value over Time')
ylabel('R Value (0-255)')
xlabel('Image')
xlim([0 90])
ylim([73 83])


subplot(2,2,3)
rgb2=rgb(y2,x2,:);
rgb3=rgb2(:).';
```

```
plot(rgb3);
title('Control Red Value over Time')
ylabel('R Value (0-255)')
xlabel('Image')
xlim([0 90])
ylim([10 20])

subplot(2,2,4)
g2=g(y2,x2,:);
g3=g2(:).';
filt = medfilt1(rgb3,10);
plot(filt);
title('Control Filtered Red Value over Time')
ylabel('R Value (0-255)')
xlabel('Image')
xlim([0 90])
ylim([10 20])
```

Appendix F. MATLAB Code Producing Absorbance Change Maps.

```
n=300; %number of images

rgb=zeros(480,640,n); %images are 480:640 res

for k = 1:n %pull the specified rgb value of each pixel over time(images)

   jpgFileName = strcat('image', num2str(k-1), '.jpg');
   imageData = imread(jpgFileName);
   rgbValue = imageData(1:480, 1:640, 2); %1=red; 2=green; 3=blue
   rgb(:,:,k)=rgbValue;

end

change = zeros(480,640,1);

for i = 1:480
   for j = 1:640
      Vector = sort(rgb(i,j,:),'descend');
      Top = Vector(1:ceil(length(Vector)*0.1));
      Bottom = Vector(ceil(length(Vector)*0.9):n);
      Delta= mean(Top)- mean(Bottom);
      change(i,j,:)=Delta;

   end

end
```

```
min_matrix = min(change(:));
max_matrix = max(change(:));

changemap=mat2gray(change, [max_matrix min_matrix]); %invert so dark corresponds to
greater change
imshow(changemap);
```

Appendix G. MATLAB Code of FFT Calculations Performed on Single Pixel.

```
n=300;

rgb=zeros(480,640,n);

for k = 1:n

    jpgFileName = strcat('image', num2str(k-1), '.jpg');
    imageData = imread(jpgFileName);
    rgbValue = imageData(1:480, 1:640, 1);
    rgb (:,:,k)=rgbValue;

end

 x=621;
 y=394;

rgb2=rgb(y,x,:);
rgb3=rgb2(:).';
plot(rgb3);
title('Absorption of 910nm over Time')
ylabel('R Value (0-255)')
xlabel('Image')

Y=fft(rgb3);

P2 = abs(Y/300);
P1 = P2(1:151);
P1(2:end-1) = 2*P1(2:end-1);
f = 30*(0:(150))/300;

figure
plot(f,P1)
xlabel('Frequency')
ylabel('Power')
title('FFT of Single Pixel')
```